HOSTED BY
ELSEVIER
CrossMark
Available online at www.sciencedirect.com
ScienceDirect
Progress in Natural Science: Materials International 25 (2015) 392–398
Progress in Natural Science Materials International
www.elsevier.com/locate/pnsmi
www.sciencedirect.com

Original research

Effect of chlorine doping on the structural, morphological, optical and electrical properties of spray deposited CdS thin films

T. Sivaraman, V. Narasimman, V.S. Nagarethinam, A.R. Balu*

PG and Research Department of Physics, A.V.V.M Sri Pushpam College, Poondi 613 503, Tamilnadu, India

Received 12 May 2015; accepted 18 June 2015
Available online 31 October 2015

Abstract

CdS and chlorine doped CdS (CdS:Cl) thin films with different Cl-doping levels (0, 2, 4, 6 and 8 at%) have been deposited on glass substrates by a spray pyrolysis technique using a perfume atomizer. The effect of Cl doping on the structural, morphological, optical and electrical properties of the films was investigated. XRD patterns revealed that all the films exhibit hexagonal crystal structure with a preferential orientation along the (0 0 2) plane irrespective of the Cl doping level. The particle size value decreases from 22.03 nm to 18.12 nm with increase in Cl concentration. Optical band gap is blue-shifted from 2.48 eV to 2.73 eV with increase in Cl doping concentration. All the films have resistivity in the order of 10^4 Ω cm. The obtained results confirm that chlorine as an anionic dopant material can enhance the physical properties of CdS thin films to a large extent.
© 2015 The Authors. Production and hosting by Elsevier B.V. on behalf of Chinese Materials Research Society. This is an open access article under the CC BY-NC-ND license (http://creativecommons.org/licenses/by-nc-nd/4.0/).

Keywords: X-ray diffraction; Crystal structure; Preferential orientation; Thin films; Optical band gap

1. Introduction

Cadmium sulfide (CdS) a direct band gap binary semiconductor is an important and useful material for photovoltaic applications [1]. Its relative wide energy band gap (2.42 eV) and n-type semiconducting characteristics make CdS a desirable window layer material for many heterojunction thin film solar cells [2]. It is well-known that native defects such as sulfur vacancies or cadmium interstitials contribute to the electrical conductivity of pure CdS. Therefore, by controlling those native defects, it is possible to enhance its electrical conductivity. It has been reported earlier that elements belonging to group III such as, indium (In^{3+}) [3], aluminum (Al^{3+}) [4], gallium (Ga^{3+}) [5], boron (B^{3+}) [6] when added to CdS as dopants can enhance its optical and electrical properties. Introduction of cationic impurities in the CdS host lattice results in the substitution of dopants in Cd sites which can enhance its opto-electronic properties. Similarly, enhanced conductivity and improved transparency can also be achieved by substituting sulfur with anionic impurities like Cl or F. Fluorine is one of the most commonly employed anionic impurities which improves the physical properties of CdS films and there are few reports on the properties of F-doped CdS thin films [7,8]. Doping and compensation of charge carriers is a notorious problem in wide bandgap compound semiconductor like CdS. Since it is generally difficult to discern the mechanism of de-activation of dopants (i.e., compensation of charge carriers) in CdS, complex methods characterizing the chemical nature, local structure, and concentration of supposed compensating defects should be applied [9]. Usually, cadmium vacancies (V_{cd}) are responsible for acceptor centers which participate in the compensation of charge carriers in CdS [10]. As the self-compensation of donors occurs through the generation of ionized cadmium vacancies [11], the highest un-compensated donor doping will be obtained for the lowest value of [V_{cd}]. So it is essential to create CdS with a decreased concentration of V_{cd} and with predetermined concentration of

*Correspondence to: 757 MIG Colony, New Housing Unit, Thanjavur 613 005, India. Tel.: +91 9442846351.
E-mail address: arbalu757@gmail.com (A.R. Balu).
Peer review under responsibility of Chinese Materials Research Society.

http://dx.doi.org/10.1016/j.pnsc.2015.09.010
1002-0071/© 2015 The Authors. Production and hosting by Elsevier B.V. on behalf of Chinese Materials Research Society. This is an open access article under the CC BY-NC-ND license (http://creativecommons.org/licenses/by-nc-nd/4.0/).

un-compensated donors like chlorine. One possible way to control the V_{cd} is the introduction of chlorine as dopant in the CdS host lattice. Maticiuc et al. [12] have reported the role of chlorine in the properties of CdS thin films prepared by chemical bath deposition. From the electrical and photoluminescence studies, they confirmed that chlorine induces some electrically and optically active defects in the CdS lattice which alters its physical properties. But details regarding the surface morphology and optical properties of CdS films due to Cl doping are not evident in their work. Besides this work, the effect of chlorine doping on the properties of CdS films is very scarce in the literature. Hence to identify the suitability of chlorine as anionic impurity replacing S in the CdS lattice, in this work chlorine doped CdS thin films were fabricated with different concentrations of chlorine (0, 2, 4, 6 and 8 at%), and a detailed investigation on the effect of chlorine on the structural, morphological, optical and electrical properties of the films is made. Amongst the different techniques used to fabricate doped CdS films, a spray pyrolysis technique using perfume atomizer is used here to fabricate Cl-doped CdS (CdS:Cl) thin films, as this technique has many advantages over the conventional spray technique such as: no need for carrier gas, fine atomization and enhanced wettability between sprayed microparticles and the previously deposited layers. Recently, we reported the effect of magnesium and zinc incorporation on the properties of CdS thin films fabricated using perfume atomizer [13,14].

2. Experimental details

The undoped CdS and Cl-doped CdS (CdS:Cl) thin films were deposited by the spray pyrolysis technique using a perfume atomizer. Chemicals used for the deposition of CdS and CdS:Cl films were cadmium chloride, thiourea and sodium chloride. All the chemicals were of analytical reagent grade (Sigma make, with a purity of 99.9%). The deposition of CdS thin films was performed on ultrasonically cleaned glass substrates (microslides of dimensions $76 \times 25 \times 1.5$ mm^3) kept at 400 °C by spraying an aqueous solution (50 ml in volume) containing 0.1 M of cadmium chloride and thiourea. Sodium chloride (NaCl) with different concentrations (0, 2, 4, 6 and 8 at%) was added to the starting solution for chlorine doping. X-ray diffraction data of undoped and Cl-doped CdS thin films were obtained with the help of a X-ray diffractometer (PANalytical – PW 340/60 Xpert PRO) with CuKα radiation ($\lambda = 1.5406$ Å) X-ray source. Surface morphological studies were carried out using a scanning electron microscope (HITACHI S-3000H). Optical transmission spectra were obtained using a UV–vis–NIR double beam spectrometer (Lambda – 35). Electrical studies were performed using a two point probe setup.

3. Results and discussion

3.1. XRD analysis

XRD patterns of CdS:Cl thin films with different Cl concentrations (0, 2, 4, 6 and 8 at%) shown in Fig. B.1 indicate their

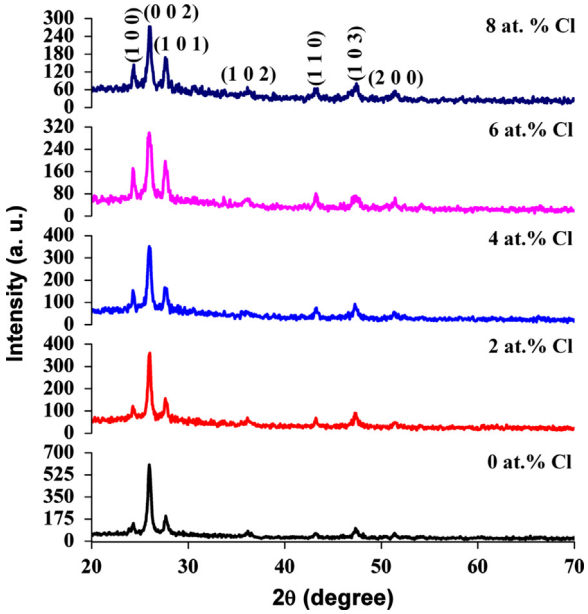

Fig. B.1. XRD patterns of CdS:Cl thin films.

polycrystalline nature. As seen, the diffraction patterns located at $2\theta = 24.3°$, 26.4°, 27.8°, 36.64°, 43.7°, 47.53° and 51.6° were indexed as (1 0 0), (0 0 2), (1 0 1), (1 0 2), (1 1 0), (1 0 3) and (2 0 0) planes respectively of hexagonal crystal structure corresponding to pure CdS (JCPDS Card no. 65-3414) with a preferred orientation along the (0 0 2) plane. No peaks corresponding to chlorine were detected in the XRD patterns, even for highest Cl doping concentration, suggesting that incorporation of Cl^- ions in the host CdS lattice does not affect its crystal structure. The degree of crystallinity for the samples decreases gradually by increasing the chlorine concentration. This could be interpreted that the doped Cl atoms prevent CdS thin film growth along or perpendicular to the substrate due to the local disorderliness created in the CdS lattice through Cl doping. This is in accordance with the results reported by Xie et al. [15] for Cu-doped CdS thin films prepared using a vacuum co-evaporation technique. The texture coefficient (TC) of the undoped and doped CdS films corresponding to the (0 0 2) plane is calculated using the formula [16]:

$$\mathrm{TC}(0\,0\,2) = \frac{\frac{I(0\,0\,2)}{I_0(0\,0\,2)}}{N^{-1}\sum_N \frac{I(hkl)}{I_0(hkl)}} \quad (1)$$

where $I(h\ k\ l)$ and $I_0(h\ k\ l)$ are the measured relative intensity and standard intensity of the $(h\ k\ l)$ plane respectively and $I(0\,0\,2)$ and $I_0(0\,0\,2)$ are the corresponding values of the (0 0 2) plane and N is the number of diffraction peaks. The calculated TC values of (0 0 2) plane are tabulated in Table A.1. It is observed that the texture coefficient falls gradually as the doping level increases, suggesting a monotonical deterioration in the crystalline quality of CdS due to Cl doping.

The diffraction peak (0 0 2) shifts towards higher 2θ value (Table A.1) with increases in Cl concentration which means a contraction in lattice volume [17]. In CdS:Cl films, Cl^- ions replaced S^{2-} ions in the host lattice, but Cl replacing ratio is

small, so CdS:Cl remained in hexagonal crystal structure of pure CdS. Due to the ionic radii mismatch between Cl^- and S^{2-}, the original inter-planar spacing decreases, so the diffraction peak shifts towards higher angle. The possible reason could be that CdS lattice gets modified and consequently its lattice parameters were altered due to Cl doping. The lattice parameters ('*a*' and '*c*') of the samples were estimated using the relation [18]:

$$\frac{1}{d^2} = \frac{4}{3}\frac{h^2+hk+k^2}{a^2} + \frac{l^2}{c^2} \quad (2)$$

and the calculated lattice parameters values are complied in Table A.1[1].

The crystallite size of the CdS:Cl thin films was calculated using the Scherrer equation [19]:

$$D = \frac{0.9\,\lambda}{\beta\,\cos\theta} \quad (3)$$

where D is the crystallite size (nm), λ is the wavelength of the X-ray (1.5460 Å), β is the full-peak width at half maximum (radians), and θ is the diffraction angle. The calculated crystallite size values are complied in Table A.2. It is observed that the crystallite size for the CdS:Cl thin films decreased from 22.03 nm to 18.12 nm with increasing Cl concentration. The crystallite size was also calculated using the Williamson–Hall (W–H) method according to the relation [20]:

$$\frac{\beta\cos\theta}{\lambda} = \frac{1}{D} + \frac{\varepsilon\sin\theta}{\lambda} \quad (4)$$

The crystallite size D was determined from the plots of ($\beta\cos\theta$)/λ versus $\sin\theta/\lambda$, where the reciprocal of the intercept on the *Y*-axis represents the crystallite size (Fig. B.2). From the Williamson–Hall results, the crystallite size of the CdS:Cl thin films decreased from 24.27 nm to 22.07 nm with increasing Cl concentration (Table A.2). The decreased in crystallite size values observed for the CdS:Cl films may be caused by the enhanced incorporation of Cl^- ions into the CdS lattice.

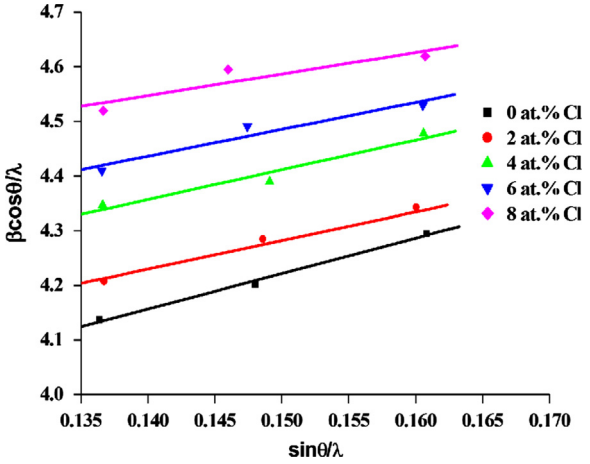

Fig. B.2. Williamson–Hall plot of CdS:Cl thin films.

3.2. SEM analysis

Fig. B.3(a)–(e) shows the SEM micrographs of CdS:Cl thin films coated with different Cl doping levels (0, 2, 4, 6 and 8 at%). The SEM micrograph of the undoped CdS thin film (Fig. B.3(a)) reveals highly porous surface with interconnected network of honeycomb. As the Cl concentration is increased to 2 at%, widened network of honeycomb disappears as evident from (Fig. B.3(b)). For 4 at% Cl doping concentration, the CdS crystal nucleus tends to grow epitaxially to form flower shaped nanostructures (Fig. B.3(c)). Similar flower structure morphology was reported by Chu et al. [21] for CdS thin films deposited by a new insitu chemical reaction synthesis using cadmium precursor as reaction source and sodium sulfide based solution as anionic reaction medium. According to them due to increased concentration of doping, CdS crystal nucleus could not form particles and they tend to grow epitaxially to form flower-like nanostructures. For 6 at% Cl doping concentration, the surface modifies with needle shaped tightly packed nanostructures (Fig. B.3(d)). However, for the film coated with 8 at% Cl doping, the surface modifies with clusters of needle shaped nanostructures (Fig. B.3(e)). These results infer that the surface morphology of CdS thin film modifies from porous surface to flower and needle shaped nanostructures with Cl doping. The modification of the surface morphology of CdS films through chlorine doping might be due to the reduction of additional structures created in the lattice due to successful diffusion of Cl^- ions. Ferra-Gonzalez et al. [22] reported that when CdS film is doped with low concentration of Ag, its surface roughness increases due to additional structures created by Ag ions. For higher doping concentration, these structures start to diffuse into the CdS lattice reducing its surface roughness.

3.3. Elemental analysis

The atomic concentrations of Cd and S as well as the S:Cd ratio obtained for the CdS:Cl films from EDS measurements are compiled in Table A.2. The S:Cd ratio of CdS as grown sample was found to be equal to 0.97, while the S:Cd ratios of CdS:Cl films with 2, 4, 6 and 8 at% Cl concentrations were found to be equal to 0.93, 0.88, 0.85 and 0.81 respectively. From EDS measurements it can be noted that chlorine incorporation reduces the sulfur atomic concentration from 37.37% to 34.23% which implies that chlorine incorporation generates sulfur deficiencies. Wan et al. [23] reported that the $CdCl_2$ annealing introduced Cl atoms into the CdS lattice which diffuse well into CdS. In the present work, the reduction of sulfur may be due to diffusion of Cl into the host lattice. The increased content of Cl observed in the EDS measurements is a supporting evidence for the incorporation of Cl into CdS. The

[1]From Table A.1, it is clear that the lattice parameters (*a* and *c*) decrease with Cl concentration, which implies that Cl^- has been incorporated into the CdS lattice replacing S^{2-} ions. As the ionic radius of Cl^- (1.81 Å) is slightly smaller than that of S^{2-}(1.84 Å), Cl^- ions can easily enter into the crystal lattice of CdS and occupy the substitutional sites, thus bringing contraction in the host lattice, which is consistent with the earlier reports on Zn-doped CdS thin films [14].

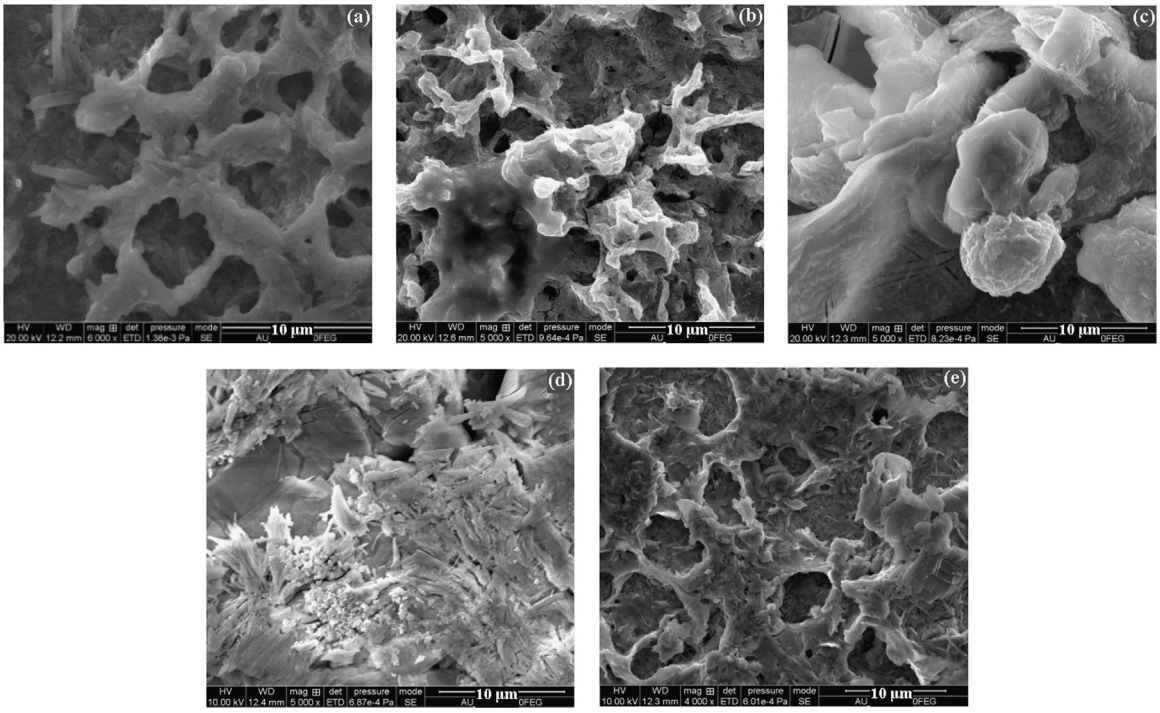

Fig. B.3. (a–e) SEM images of CdS:Cl thin films.

other peaks seen in Fig. B.4 are related to the substrate elements.

3.4. Optical studies

Fig. B.5 shows the optical transmittance spectra of undoped and Cl-doped CdS films. The undoped CdS film has a transmittance about 78% in the wavelength range 500–700 nm. In this same wavelength range, CdS films with chlorine concentrations 2, 4, 6 and 8 at% have a transmittance of about 80%, 84%, 87%, and 90% respectively. Thus Cl doped CdS samples show a significant increase in the transmittance when compared to the undoped film. The higher transmittance indicates lower defect density and better electrical properties of the CdS:Cl films because of absorption of light in the longer wavelength region (>500 nm) which is usually caused by crystalline defects such as grain boundaries and dislocations [24]. As seen in Fig. B.5, the absorption edge of CdS:Cl films shifts towards lower wavelength side with increase in Cl doping concentration which indicates that the optical band gap of CdS:Cl films should increase. The band gap energy of the films is calculated using the Tauc's relation:

$$\alpha h\nu = A\left(h\nu - E_g\right)^n \quad (5)$$

where A is a constant, $h\nu$ is the incident photon energy, α is absorption coefficient, E_g is the band gap energy of the films, and n is equal to ½ for allowed direct transition. The optical band gap of CdS:Cl films is calculated by extrapolating the straight line portion of the plots of $(\alpha h\nu)^2$ versus photon energy ($h\nu$) shown in Fig. B.6 to the energy axis at $\alpha=0$. The determined band gap value of undoped CdS film was found to be equal to 2.48 eV. The obtained band gap value exactly matches with the value obtained by Shah et. al [25] for CdS films fabricated by a close spaced sublimation technique. The E_g value obtained for the undoped CdS film is slightly higher than the energy gap for bulk CdS (2.42 eV). This blue-shift in the band gap value is due to a quantum size effect as reported by Mahdi et al. [26]. The band gap values of CdS:Cl films coated with 2, 4, 6 and 8 at% Cl concentrations were found to be equal to 2.55, 2.62, 2.68 and 2.73 eV respectively. The higher band gap values observed for the Cl-doped CdS films may probably be due to the occupacy of Cl atoms in the CdS lattice and the quantum size effect as expected for the nanocrystalline nature of the films, which means that Cl-doped CdS thin films enable much more ray of light of shorter wavelength to transit, making it helpful in improving solar cell efficiency. Increased band gap values observed for the doped films might also be due to the decreased crystallite size values observed (Table A.2), which lead to quantum confinement of the charge carriers in the crystallites which result in the increase of a band bending effect, the degree of preferred orientation, internal microstrain and stoichiometry [27]. In nano-crystalline materials, the band bending effect can be expected at the grain boundaries as the surface to volume ratio is higher. Normally, in crystallites with smaller size, the band bending effect will be more compared to bigger crystallites. Owing to quantum confinement, the band gap increases due to reduced crystallite size, which result in the shift of absorption threshold to shorter wavelength due to individual confinement of electrons and holes. The energy gap broadening may also be related to the existence within the band gap of a high density levels with energies near the bands, which can give rise to band tailing as has been suggested for many polycrystalline materials. This is in accordance with the results reported by

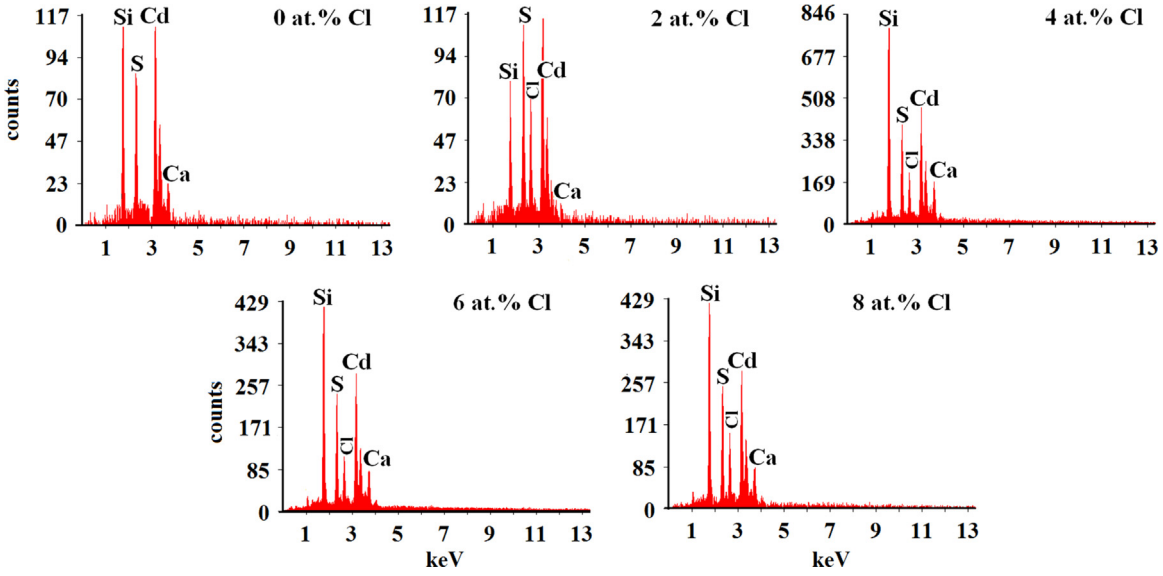

Fig. B.4. EDAX spectra of CdS:Cl thin films.

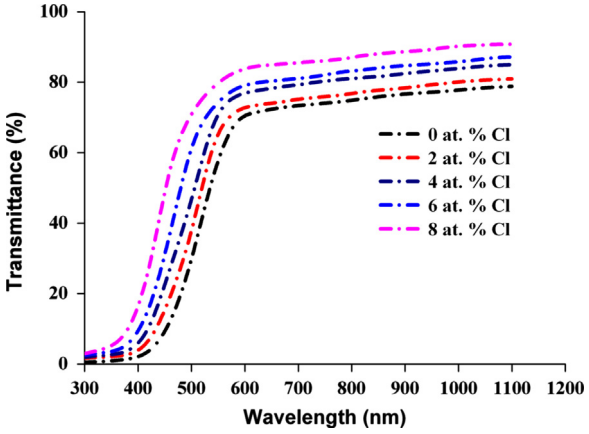

Fig. B.5. Transmittance spectra of Cl-doped CdS films.

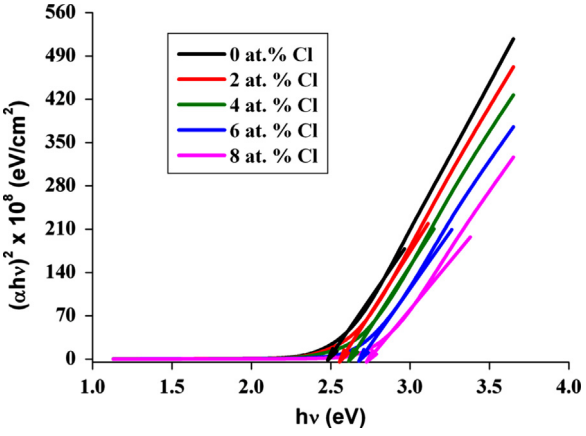

Fig. B.6. Tauc's plots of CdS:Cl films.

Rajashree et al. [28] for Cd-doped PbS thin films. There are few reports on the variation in the band gap of CdS films after doping with metallic ions such as Mg [13], In [29], etc. and with non-metallic ions such as F [8]. Podesta et al. [7] reported that doping CdS with anionic impurity fluorine can enhance its band gap. The blue-shift phenomenon of E_g observed here (band gap widening) with Cl doping could also be attributed to the so-called a Moss–Burstein effect [30], in which the optical absorption is shifted towards higher energy by an amount proportional to the free-electron density. The fact that the onset of light absorption is shifted towards lower wavelengths in thin films, especially doped ones, turns to be advantageous for optical applications in the UV [31]. The wide band gap and high optical transparency observed for the CdS:Cl films make them possible window layers in solar cell applications.

The refractive index n is an important physical parameter related to microscopic atomic interactions. There are theoretically two different approaches in viewing this subject: i) the refractive index related to density and ii) the local polarizability of these entities [32]. Based on the representation of crystalline structure by a delocalized picture, n will be closely related to the energy band structure of the material. Many attempts have been made to relate the refractive index and the energy gap E_g through simple relationships and a few will be reviewed here to validate the current work. The linear relationship between refractive index n and E_g is represented as [33]:

$$n = \alpha + \beta E_g \tag{6}$$

where $\alpha = 4.048$ and $\beta = -0.62\ \mathrm{eV}^{-1}$

Herve and Vandamme [34] had proposed an empirical relation between n and E_g as:

$$n = \sqrt{1 + \left(\frac{A}{E_g + B}\right)^2} \tag{7}$$

where $A = 13.6$ eV and $B = 3.4$ eV

Ghosh et al. [35] considering the band structure and quantum-dielectric formulations of Penn [36] and Van Vechten

[37] formulated an expression for the high frequency refractive index as

$$n^2 - 1 = \frac{A}{(E_g + B)^2} \quad (8)$$

where $A = 25E_g + 212$ (concentration from the valance electrons), $B = 0.21E_g + 4.25$ a constant additive to the lowest band gap E_g and $(E_g + B)$ refers to an appropriate energy gap of the material.

Thus, these three models of variation of n with energy gap have been calculated. The calculated refractive index values are compiled in Table A.3[2].

3.5. Electrical studies

The electrical resistivity measurements showed that CdS:Cl films have resistivity in the order of 10^4 Ω cm. The order of resistivity obtained here exactly matches with the values reported by Hiie et al. [40] for CdS thin films prepared by chemical bath deposition. For undoped CdS films, the resistivity is found to be 2.35×10^4 Ω cm. For the CdS:Cl films, the calculated resistivity values were found to be equal to 1.88×10^4 Ω cm, 0.469×10^4 Ω cm, 0.164×10^4 Ω cm and 0.094×10^4 Ω cm for the films with 2, 4, 6 and 8 at% Cl concentrations respectively. The reduction in the resistivity of CdS:Cl films is due to increased carrier concentration due to substitutional incorporation of Cl^- ions in the CdS structure. Also the reduction of the resistivity can be attributed to the rise of carriers due to sulfur deficiencies [41], which agrees with the compositional analysis. It can be observed from EDS analysis (Table A.2), that sulfur vacancies (V_s) increases whereas Cd vacancies (V_{cd}) decreases with increasing Cl concentration. As the doping concentration increases, annihilation of V_{cd} (acceptor centers) and V_s (donors) takes place with a beneficial situation being created for the incorporation of Cl atoms on the unoccupied V_s sites, thereby increasing the electron concentration which results in the decrease in the resistivity of the doped films, with increased content of Cl.

4. Conclusion

Nanostructured CdS:Cl thin films were deposited by the spray pyrolysis technique using a perfume atomizer with 0, 2, 4, 6 and 8 at% Cl concentrations. XRD studies revealed that all the films exhibited hexagonal crystal structure with a (0 0 2) preferential orientation. The diffraction peak (0 0 2) shifts towards higher 2θ value with increase in Cl concentration. Film transparency increases with increase in Cl concentration. Optical studies showed that the band gap values of CdS:Cl films suffered a blue-shift with increase in chlorine concentration. For all the doped films electrical resistivity decreased with increase in Cl concentration. High transparency and low resistivity values obtained for the CdS:Cl films make them suitable for opto-electronic devices, especially as window layer for solar cell applications. The obtained results infer that chlorine might be a good anionic dopant material which can enhance the physical properties of CdS thin films.

[2]The calculated refractive index values are in good agreement with the experimental value [38]. It is observed that the refractive index value decreases with Cl doping concentration which might be due to the lower refractive index of Cl (approximately equal to 1). Another reason for the decrease in refractive index might be due to the changes in internal structure of CdS which cause the decrease in the propagation velocity of light. This is in accordance with the Han et al. [39] for Co doped CdS thin films.

Table A.1
2θ, d-spacing, texture coefficient (TC) and lattice parameters of CdS:Cl films.

Cl doping concentration (at%)	$2\theta^*_{(0\ 0\ 2)}$ (deg)	$d^*_{(0\ 0\ 2)}$	TC(0 0 2)	Lattice parameters		
				$a^* = b$ (Å)	c^*(Å)	c/a
0	25.961	3.3678	7.28	4.1250	6.7356	1.6329
2	25.963	3.3676	7.23	4.1244	6.7352	1.6330
4	25.965	3.3675	7.14	4.1243	6.7350	1.6330
6	25.968	3.3673	6.86	4.1241	6.7346	1.6330
8	26.001	3.3670	7.10	4.1237	6.7340	1.6330

Standard values $*2\theta = 26.45^\circ$; $d = 3.3670$ Å; $a = 4.1320$ Å; $c = 6.7340$ Å (JCPDS Card no.: 65-3514)

Table A.2
Crystallite size and elemental composition of CdS:Cl thin films.

Chlorine doping level (at%)	Crystallite size, D (nm)		Elemental composition (at%)			
	From XRD	From W–H plots	Cd	S	Cl	S:Cd
0	22.03	24.27	38.41	37.37	–	0.97
2	21.97	23.80	39.65	36.86	3.17	0.93
4	21.38	23.09	40.98	36.05	5.60	0.88
6	20.03	22.67	41.12	35.14	6.02	0.85
8	18.12	22.07	42.02	34.23	7.72	0.81

Table A.3
Band gap energy (E_g) and refractive index (n) values of CdS:Cl films calculated using Ravindra et al. [33], Herve and Vandamme et al. [34] and Ghosh et al. [35] models of CdS:Cl thin films.

Sample	Band gap, E_g (eV)	Refractive index		
		n^a	n^b	n^c
0 at% Cl	2.48	2.554	2.5454	2.510
2 at% Cl	2.55	2.523	2.528	2.497
4 at% Cl	2.62	2.486	2.506	2.482
6 at% Cl	2.68	2.386	2.450	2.443
8 at% Cl	2.73	2.293	2.401	2.409

[a]Ref. [33].
[b]Ref. [34].
[c]Ref. [35].

Acknowledgments

The authors are thankful to the Head, Department of Physics, Mr. Karthik, Alagappa University, Karaikudi for the

XRD analysis, Head, Department of Chemistry and Mr. Gowtham, Gandhigram Rural Institute, Dindugal for the SEM and EDAX measurements.

Appendix A

See Tables A.1–Tables A.3.

References

[1] G. Perna, V. Capozzi, M. Ambrico, V. Ligonze, A. Minafra, L. Schiavulli, M. Pallara, Thin Solid Films 453 (2004) 187–194.
[2] H. Chavoz, M. Jordan, J.C. McClure, G. Lush, V.P. Singh, J. Mater. Sci. Mater.: Electron. 8 (1997) 151–154.
[3] D. Acosta, C. Magana, A. Martinez, A. Maldonado, Sol. Energy Mater. Sol. Cells 82 (2004) 11–20.
[4] B. Patil, D. Naik, V. Shrivastava, Chalcogenide Lett. 8 (2011) 117–121.
[5] H. Khallaf, G. Chai, O. Lupan, L. Chow, S. Park, A. Schulte, Appl. Surf. Sci. 255 (2009) 4129–4134.
[6] J. Lee, J. Yi, K. Yang, J. Park, R. Oh, Thin Solid Films 431 (2003) 344–348.
[7] A. Podesta, N. Armani, G. Salviati, M. Romeo, A. Bosio, M. Prato, Thin Solid Films 511 (2006) 448–452.
[8] F. de Moure-Flores, K.E. Nieto-Zepeda, A. Guillen-Cervantes, S. Gallardo, J.G. Quinones-Galvan, A. Hernandez-Hernandez, M. de la, L. Olvera, M. Zapata-Torres, Yu Kundriavstev, M. Melendez-Lira, J. Phys. Chem. Solids 74 (2013) 611–613.
[9] U.V. Desnica, I.D. Desnica-Frankovie, R. Magerle, A. Buchard, M. Deicher, J. Cryst. Growth 197 (1999) 612–615.
[10] M. Aven, J.S. Prener., Physics and Chemistry of II–VI Compounds, General Electric Research and Development Center, Scheneclady, New York, 1967.
[11] Y. Marfaing, Thin Solid Films 387 (2001) 123–128.
[12] N. Maticiuc, J. Hiie, T. Raadik, A. Graf, A. Gavrilov, Thin Solid Films 535 (2013) 184–187.
[13] T. Sivaraman, A.R. Balu, V.S. Nagarethinam, Mater. Sci. Semicond. Process. 27 (2014) 915–923.
[14] M. Anbarasi, V.S. Nagarethinam, A.R. Balu, Mater.Sci-Pol. 32 (2014) 652–660.
[15] H. Xie, C. Tian, W. Li, L. Feng, J. Zhang, L. Wu, Y. Cai, Z. Lei, Y. Yang, Appl. Surf. Sci. 257 (2010) 1623–1627.
[16] K. Usharani, N. Raja, N. Manjula, V.S. Nagarethinam, A.R. Balu, Int. J. Thin Films Sci. Technol. 4 (2015) 89–96.
[17] N. Badera, B. Godbole, S.B. Srivastava, P.N. Vishvakarma, L.S. Sharath Chandra, D. Jain, M.G. Angrade, T. Shripati, V.G. Sathe, V. Ganesan, Appl. Surf. Sci. 254 (2008) 7042–7048.
[18] T. Sivaraman, A.R. Balu, V.S. Nagarethinam, Res. J. Mater. Sci. 2 (2014) 6–15.
[19] A.R. Balu, V.S. Nagarethinam, A. Thayumanavan, K.R. Murali, C. Sanjeeviraja, M. Jeyachandran, J. Alloy. Compd. 502 (2010) 434–438.
[20] N. Choudhury, B.K. Sarma, Bull. Mater. Sci. 32 (2009) 43–47.
[21] J. Chu, Z. Jin, W. Wang, H. Liu, D. Wang, J. Yang, Z. Hong, J. Alloy. Compd. 517 (2012) 54–60.
[22] S.R. Ferra-Gonzalez, D. Berman-Mendoza, R. Garcia-Gutierrez, S. J. Castillo, R. Ramirez-Bon, B.E. Gnade, M.A. Quevedo-Lopez, Optik 125 (2014) 1533–1536.
[23] L. Wan, Z. Bai, Z. Hou, D. Wang, H. Sun, L. Xiong, Thin Solid Films 518 (2010) 6858–6865.
[24] J.Y. Choi, K.J. Kim, J.B. Yoo, D. Kim, Sol. Energy 64 (1998) 41–47.
[25] N.A. Shah, R.R. Sagar, W. Mahmood, W.A.A. Syed, J. Alloy. Compd. 512 (2012) 185–189.
[26] M.A. Mahdi, Z. Hassan, S.S. Ng, J.J. Hassan, S.K. Mohd. Bakhori, Thin Solid Films 520 (2012) 3477–3484.
[27] J.P. Enriquez, X. Mathew, Sol. Energy Mater. Sol. Cells 76 (2003) 313–322.
[28] C. Rajashree, A.R. Balu, V.S. Nagarethinam, Surf. Eng. 31 (2015) 316–321.
[29] T.D. Dzhafarov, F. Ongul, S. Aydin Yuksel, Vacuum 84 (2010) 310–314.
[30] A.A. Dakhel, Sol. Energy 82 (2008) 513–519.
[31] A.V. Moholkar, G.L. Agawane, Kyu-Ung Sim, Ye-bin Kwon, K. Y. Rajpure, J.H. Kim, Appl. Surf. Sci. 257 (2010) 93–101.
[32] N.M. Balzaretti, J.A.H. daJornad, Solid State Commun. 99 (1996) 943–948.
[33] N.M. Ravindra, S. Auluck, Y.K. Srivastave, Phys. Status Solidi 6 (1979) 155–160.
[34] P.J.L. Herve, L.K.J. Vandamme, J. Appl. Phys. 77 (1995) 5476–5477.
[35] D.K. Ghosh, L.K. Samanta, G.C. Bhar, Infrared Phys. 24 (1984) 43–47.
[36] D.R. Penn, Phys. Rev. 128 (1962) 2093–2097.
[37] J.A. Van Vechten, Phys. Rev. 182 (1969) 891–905.
[38] R.C. Weast, Handbook of Chemistry and Phyics, 53, CRC Press, Florida, 1972.
[39] Yan-Xiao Han, Chuan-Lu Yang, Yong-Tai Sun, Mei-Shan Wang, Xiao-Guang Ma, J. Alloy. Compd. 585 (2014) 503–509.
[40] J. Hiie, T. Devoda, V. Valdsa, K. Muska, Thin Solid Films 511 (2006) 443–447.
[41] O. de Melo, L. Hernandez, O. Zelaya-Angel, R. Lozado-Morales, M. Becerril, E. Vasco, Appl. Phys. Lett. 65 (1994) 1278–1280.